Biodegradable Mg implants: how to improve the surface properties?

T. Journot¹, C. Csefalvay¹, O. Banakh¹, A. Cornillet², D. Stephan², B. Schnyder²

¹ Haute Ecole Arc Ingénierie (HES-SO), La Chaux-de-Fonds, CH, ² HES-SO Valais, Sion, CH

INTRODUCTION: Due to their ability to resorb in the human body and to provide specific biological responses, Mg-based implants can be classified as bioactive and biodegradable materials. In the past decades, they were successfully used as cardiovascular and orthopedic implants. To provide mechanical integrity in the body over several months, the corrosion process must be precisely controlled. Plasma Electrolytic Oxidation (PEO) surface treatment has been proven an efficient method for corrosion protection of Mg alloys. We showed how PEO improves the corrosion resistance of AZ31. Different post-treatments improving biological properties of the Mg alloys can be considered in the fabrication chain of future resorbable implants.

METHODS: Polished AZ31 discs (30 mm diam.) were anodized by PEO using a CIRTEM® bipolar pulsed current source (f=100 Hz; J+= $30 \div 60 \text{ A/dm}^2$, J= $0 \div 30 \text{ A/dm}^2$). The electrolyte contained 4 g/l NaOH and 6.3 g/l calcium glycerophosphate (pH=12.5). Treatment time was 5 min resulting in the anodized layer thickness of 15-20 µm. Two post-treatments were performed after PEO: 1) 50 nm-thick TiO₂ layer was deposited by Atomic Layer Deposition (ALD) and 2) a PLLA (poly-L-lactic acid) layer (10 µm-thick) was deposited by dip-coating. The surface and cross-section morphology were examined by Scanning Electron Microscopy (SEM) and optical microscopy. Corrosion tests were performed by potentiometry. Hydrogen gas evolution was measured by immersing the samples in HCl (0.25 M) solution. Biological assays with mouse fibroblast L929 cells were performed on the treated samples in order to assess their cytocompatibility. L929 cells were grown in contact with sample extracts, degraded during 24 and 72 hours in DMEM/F12 medium supplemented with 10 % FCS and 1 % PenStrep. WST-8 proliferation assays were used to assess cell viability in presence and absence of the coated sample extracts. Cell viability in absence of the sample was taken as 100 % viability.

RESULTS: The surface of anodized samples presents a morphology typical for PEO layers, showing a high percentage of open pores originating from arc discharges and gas emission through the growing PEO layer (Fig. 1, left). The potentiometry results show that PEO treatment enhanced the corrosion resistance by a factor of 300 (compared to non-treated AZ31). The emission of hydrogen gas, resulting from a reaction between Mg and HCl, was significantly retarded by PEO treatment. No hydrogen bubbles were observed during first 30 days of tests for PEO-treated samples, while 250 mL of gas was collected after 15 min of test with untreated AZ31 sample (same test conditions).

The results of biological tests indicated a poor cell viability for PEO-treated AZ31. The cell viability increased significantly (> 80%) after ALD post-treatment (Fig.1, right). PLLA coating resulted in a cell viability of 60% (compared to the reference).

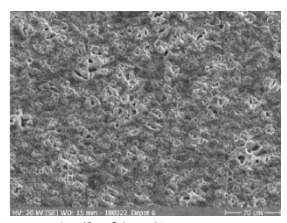




Fig. 1 (left): SEM image of the surface of PEO-treated AZ31; (right): optical microscopy image (200x) of L929 cells exposed during 24 h to the PEO-ALD sample.

DISCUSSION & CONCLUSIONS: PEO is a suitable surface treatment enhancing the corrosion resistance of Mg-based alloys. However, open pores in the PEO layer are problematic as they could initiate Mg ion release from the substrate in contact with a physiological medium, resulting in a pH increase in the surrounded area and poor biological response. Post-treatments (TiO₂ by ALD, dip-coating with PLLA) can further improve the corrosion resistance of the PEO-treated Mg alloys. They are necessary to obtain a favourable biological response in contact with viable cells.

Multilayer coating based on parylene-C and TiO₂ deposited by ALD for the packaging of medical devices

<u>D. Grange</u>, N. Chatelain, S. Farine-Brunner, L. Jeandupeux, T. Journot *Haute Ecole Arc Ingénierie (HES-SO), La Chaux-de-Fonds, CH*

INTRODUCTION: Implantable electronic devices intended to stay over long periods of time in the human body must be protected from the physiological environment by means of an encapsulation to avoid their failure during the use and achieve the highest longevity.

This encapsulation must be mechanically stable (to avoid damage due to, e.g. liquid infiltration that causes corrosion of the device), biocompatible, and have a high corrosion resistance. Our new multilayer coating showed promising results as a conformal packaging layer.

METHODS: This study aims to develop a thin encapsulation coating combining poly(chloro-p-xylylene) (commercial name parylene-C) layers with a thickness of 500 nm deposited by LPCVD, and 15 nm TiO₂ layers deposited by Atomic Layer Deposition (ALD) using tetrakis(dimethylamido)titanium (Ti[N(CH₃)₂]₄) and water as precursors with a process time of 8 hours maximum and a process temperature as low as possible.

The barrier performance of the layers has been tested by three different means: helium leak test, immersion of coated magnesium samples in Ringer's solution and immersion of coated Nd-Fe-B magnets in Ringer's solution.

The layers have been tested individually and combined by changing the order of the two layers and the number of alternation.

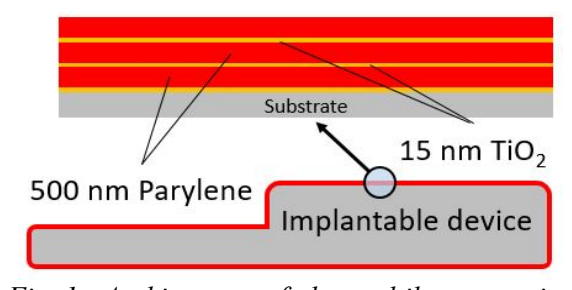


Fig. 1: Architecture of the multilayer coating composed of TiO₂ deposited by ALD and parylene-C deposited by LPCVD.

The optimized multilayer coating consists of 3 TiO₂ layers (15 nm-thick) alternating with 3 parylene-C layers (500 nm-thick) all deposited at a low temperature (50 °C) (Fig. 1). It exhibited

a protection comparable to a 3 times thicker state of the art commercial barrier coating.

RESULTS: We noticed that parylene-C was damaged by an ALD process above 50 °C. Indeed, the permeability of a multilayer with TiO₂ deposited at 150 °C is higher than that of parylene alone or multilayer with TiO₂ deposited at 80 °C or 50 °C.

Moreover, barrier properties of TiO₂ deposited at 50 °C are as good as those of TiO₂ deposited at 80 °C or even at 150 °C (for the same layer thickness).

Finally, the optimized multilayer coating with a total thickness of 1.6 μ m showed better or equivalent results in most of the tests than the commercial state of the art multilayer coating with a total thickness of 5 μ m (Fig. 2).

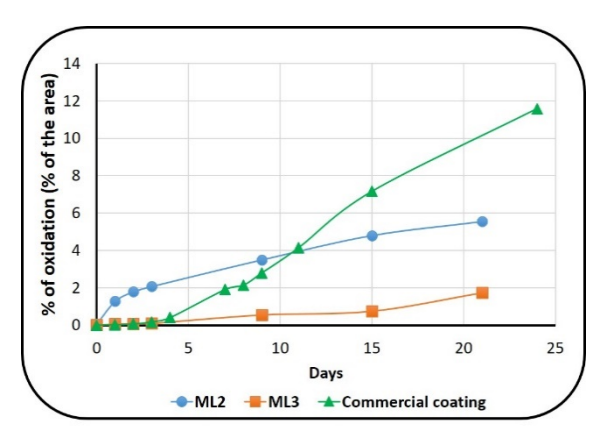


Fig. 2: Evolution of the oxidized area of coated Mg samples immersed in Ringer's solution: a multilayer made of 2 alternations (ML2), 3 alternations (ML3) and the commercial barrier coating.

DISCUSSION & CONCLUSIONS: The optimized multilayer coating showed excellent barrier properties with a thickness less than 2 μm. Nevertheless, progress has to be made in term of reproductively. Changing of reactor for every layer is detrimental. Therefore replacement of parylene-C by another material deposited by ALD is envisaged.

ACKNOWLEDGEMENTS: We would like to thank the HES-SO for its financial support in the frame of project "PolyPackAL".

MRI compatibility of additive manufactured auxetic NiTi parts

F. Schuler¹, I. Brumer², A. Adlung², TP. Pusch³, M. Siegfarth^{2,3}, P. Renaud⁴, M. de Wild¹

¹ <u>FHNW</u> Muttenz, CH, ² Computer Assisted Clinical Medicine, Medical Faculty Mannheim,

Heidelberg University, Mannheim, DE, ³ Fraunhofer Institute for Manufacturing Engineering

and Automation, Mannheim, DE, ⁴ INSA-<u>ICUBE</u>, Strasbourg, FR

INTRODUCTION: In the context of the SPIRITS project a 3D-printed design of an assistance robot for interventional surgery under Magnetic Resonance Imaging (MRI) is developed^{1,2}. It is of the outmost importance that the manufactured components do not affect the image quality³. Artefacts in imaging could be caused on one hand by eddy currents due to the numerous loops of the auxetic structure (Fig. 1), and on the other hand by the nickel-containing shape memory alloy NiTi consisting of approx. 50 % Ni, which is ferromagnetic in its elementary form³.

METHODS: Auxetic structures printed using selective laser melting (SLM) in medical degree pure titanium (strut thickness $s = 500 \mu m$) and a NiTi alloy ($s = \sim 600 \mu m$) were compared. Images were acquired with artefact susceptible TRUFI sequences at 3 T (Magnetom Skyra, Siemens Healthineers, Germany)



Fig. 1: CAD view of an auxetic structure (\$\pi 30\$ mm, \$h=50\$ mm).

RESULTS: All 3D-printed metallic structures could be mapped without any significant side effects such as heating, movement or intense disturbing image artefacts. It was found that NiTi structures lead to slightly larger artefacts than Ti (Fig. 2 and Fig. 3).

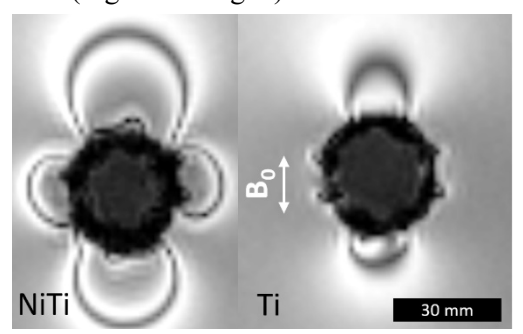


Fig. 2: MRI images of NiTi and Ti structures.

Furthermore, the signal inside both structures is significantly reduced by the induced eddy currents. The observed artefacts are primarily expressed radially in the direction of the main magnetic field B_{θ} .

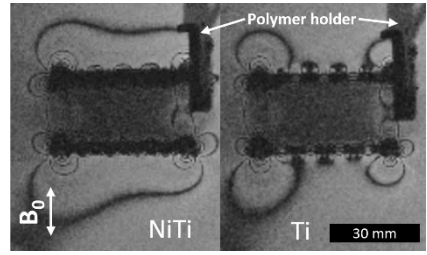


Fig. 3: MRI images of NiTi and Ti structures.

DISCUSSION & CONCLUSION: The observed imaging artefacts can be considered non-problematic due to the region of interest being in axial direction, outside of the auxetic structure. The reason for the major disturbances around the NiTi actuators could be the material difference but also the slightly thicker realization of the structures. Based on the observed behavior, no critical design flaw was identified.

REFERENCES: 1 W. Neumann, T.P. Pusch, M. Siegfarth, L.R. Schad, J.C. Stallkamp. CT and MRI compatibility of flexible 3D-printed materials for soft actuators and robots used in image-guided interventions. Med Phys. 2019;46(12):5488-5498. ² A. Pfeil A, L. Barbé, B. Wach, A. Bruyas, F. Geiskopf, Nierenberger, et al. A 3D-Printed Needle Driver Based on Auxetic Structure and Inchworm Kinematics. **ASME IDETC** V05AT07A057. ³ A. Melzer, S. Michitsch, S. Konak, G. Schaefers, T. Bertsch. Nitinol in magnetic resonance imaging, Minim Invasive Ther Allied Technol. 2004;13(4):261-71.

ACKNOWLEDGEMENTS: The SPIRITS project is supported by the Region Grand Est, Land Baden-Württemberg, Land Rheinland-Pfalz, Cantons Baselstadt, Basellandschaft, Aargau, Swiss Confederation and by the program INTERREG Upper Rhine from the ERDF (European Regional Development Fund).

Protection of Electronics for Reprocessable Surgical Devices

G. Schaffner

Turck duotec SA, Delémont, CH

INTRODUCTION: Electronics destined to be placed in a reusable surgical device will likely have to go through reprocessing (commonly cleaning followed bv machine sterilization) prior to a subsequent surgical procedure. Reprocessing is known to be very aggressive on electronics (even when protected) because of the temperature, pressure and chemicals involved. Protection of electronics through overmolding can be done by polymeric materials (despite their lower barrier effect properties compared with metals) as a result of the quasi absence of gaps, i.e. no microclimate inside of the housing. The risk of condensing of unwanted chemicals (mostly water after sterilization) is drastically reduced. Unlike the involved chemicals in gaseous phases that are relatively harmless for an overmolded electronic device, the chemicals in liquid phase (cleaning products, typically solutions of very strong bases, pH 11 and more) are chemically very aggressive and are to be reliably kept off of the electronics even after several reprocessing cycles. This article discusses this specific topic in the case of an overmolded electronic device.

METHODS: Overmolding allows to build a housing in one block and in one-step process around an electronic device. Except from the interface between the connection elements (typically fluor-polymer isolated conductors or golden pins) and the overmolding material, there aren't any potential ingress paths for a liquid. It is commonly known that interfaces are prone to ageing and to a delamination throughout the repeated reprocessing cycles.

In this study, we tested the sealing quality of an overmolded electronic device equipped with PTFE conductors. The PTFE conductors had been pre-treated in order to improve their adherence potential with the overmolding material. The testing method was to perform a dielectric test after an IP67 immersion in water at different ageing stages.

Ageing is performed in the air, inside a thermal shock chamber from 0 °C to 150 °C. The sterilization temperature range is typically from 20 °C to 135 °C. The extended temperature range for the ageing is meant to compensate for

the higher thermal conduction coefficient of steam compared to air. Alternatively, another group of parts was aged inside of a tabletop sterilizer running in a loop. The sterilizer used for the test didn't completely cool down to room temperature at the end of each cycle, leading to a degraded test.

To test the sealing against the IP 67 standard, the samples have to be immersed for 30 minutes in water over-pressurized with 0.1 bar. The method for detecting potential water ingress into the housing is a dielectric test at 1500 volt performed in water. If the leakage current stays underneath the limit of 0.350 mA, the test is successful (see IEC 60947-1, §8.3.3.4)

RESULTS: Figure 1 shows the values of the dielectric test after an IP 67 immersion and after different ageing stages. The two different groups of parts tested (up to 556 sterilizations at 134 °C and aged up to 800 thermal shocks from 0 to 150 °C) are represented in black and grey. Both values are at least ten times below the acceptance criteria for this test. The outliner (part N°2) was defective from the beginning. After analysis, the root cause was a damaged conductor, outside of the overmolding area.

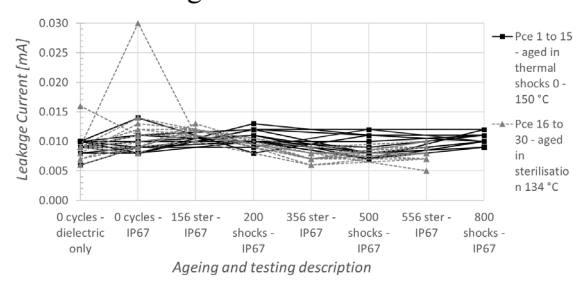


Fig. 1: Leakage current after an IP67 immersion in water and different ageing stages.

DISCUSSION & CONCLUSIONS: The results show a very low and stable leakage current, proving the sealing-performance between the PTFE and overmolding material interface in harsh environments. Additional tests also have been conducted in real environments (over a thousand machine cleanings plus steam sterilization cycles) without any failure of the electronic, which confirms the laboratory results. Similar work is currently in progress to study the performance of pre-treated gold pins in overmoldings.

Surface Properties and Fatigue Resistance of AM-Structures

R. Heuberger, A. Butscher

RMS Foundation, Bettlach, CH

INTRODUCTION: Additive manufacturing (AM) is a promising technology that allows revolutionary possibilities such as "complexity for free". In contrast, the physical properties of these components are often neither known nor assessable. This entails new risks and challenges with regard to the quality and reliability of such products, especially for applications in medical technology.

METHODS: Simulating a 3D-structure for better bone attachment on an acetabular cup, a special grid structure made of the titanium alloy Ti6Al4V was deposited on bars made of the same alloy using laser metal deposition (1.9 mm high structure on 60 x 10 x 5 mm bar, produced at Fraunhofer Institute for Laser Technology ILT, Aachen, D). Surface properties of these structures were investigated using confocal microscopy and scanning electron microscopy (SEM). The fatigue resistance was subsequently investigated using a 4-point bending test (270 - 637 MPa, 10 Hz). Finally, a fracture analysis was performed on the tested samples.

RESULTS: The surface analysis showed small metallic droplets on the surface of the AM-structures. The roughness Ra of the structures ranged from 0.11 to $1.2 \mu m$.

There was an early failure of the bars with the AM-structures in the 4-point bending test (< 300'000 cycles at 270 MPa vs. > 700'000 cycles at 600 MPa for Ti-bars w/o structure). The SEM-investigation showed multiple crack initiation within the AM-structure (Fig. 1 & 2).

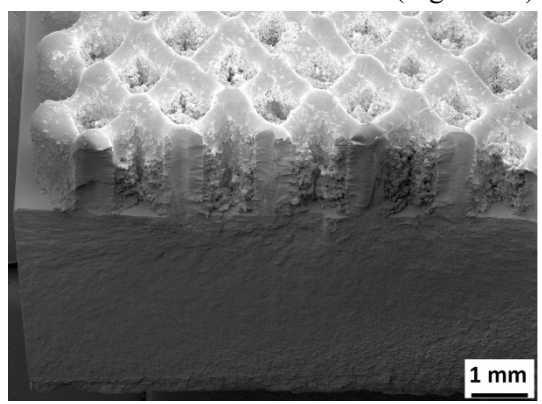


Fig. 1: SEM-image of the fracture surface. The AM-structure was deposited on a bar by laser metal deposition.

The metallographic examination of the broken samples showed additional secondary cracks that start at the interface (Fig. 3). The microstructure of the AM-structure and of the heat affected zone at the interface was dendritic, while the bar exhibited small grains. The AM-structures were harder than the bulk (389 \pm 2 vs. 322 \pm 10 HV $_{0.5}$). This was related to a higher oxygen content in the AM-structure.

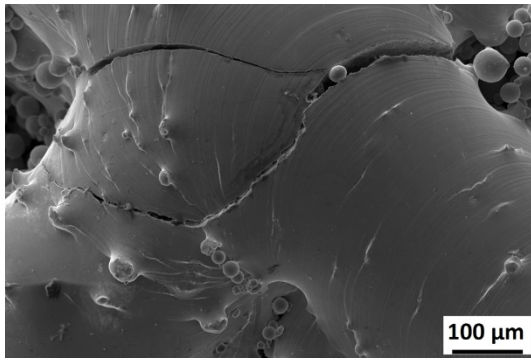


Fig. 2: SEM-image of the AM-structure with secondary cracks.



Fig. 3: Optical image of an etched cross-section to reveal the grain structure. The arrow points on a secondary crack at the interface.

DISCUSSION & CONCLUSIONS: The reason for the failure was the higher hardness due to a higher oxygen content of the AM-structures compared to the bulk material. Thus the upper part was more brittle than the bulk. This led to cracks in the AM-structure and at the interface, and finally to the early failure of the components due to the cyclic bending stress and notch sensitivity.

This example shows that application specific testing and analysis can be crucial for product failure prevention.

Accelerated tests for lifetime prediction of interfaces and interlayers with respect to crevice and fatigue corrosion in body fluid

R. Hauert¹, E. Ilic¹, A. Pardo¹, M. Stiefel¹, S. Mischler², P. Schmutz¹

¹ Empa, Swiss Federal Laboratories for Materials Science and Technology, Dübendorf, CH. ² EPFL, Tribology and Interfacial Chemistry Group, Lausanne, CH

INTRODUCTION: Coatings have an interface with the substrate where a few nanometer reactively formed material is generated with different properties compared to those of the coating or the substrate. Depending on the processing conditions, contaminations in the range of one atomic layer may be present, which can result in altered corrosion and fatigue behavior of this particular interfaces.

METHODS: To measure the chemical composition and reactivity of the nm-thick interface material, the coated sample was polished by an ion beam at an ultralow angle. Then, Auger Electron Spectroscopy (AES) characterized measurements locally the composition and microcapillary electrochemical measurements determined the local reactivity [1]. Crevice corrosion, which is not accelerated in a physiological implant simulator, was accelerated in a dedicated crevice/confined space setup [2]. Corrosion fatigue testing of an interface in articulating simulator testing only lead to a good/bad result. By reciprocal sliding over a coating in media, an alternating load was generated at the interface. This test methodology did generate the Wöhler curve and the corresponding endurance limit of a particular interface [3].

RESULTS:

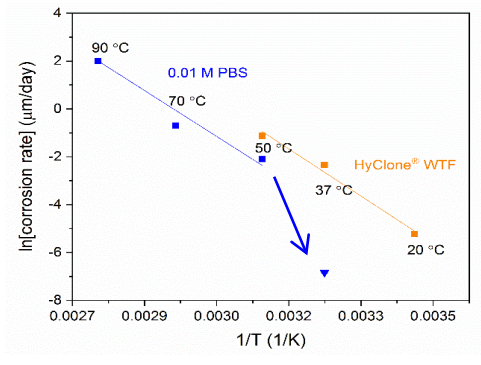


Fig.1: Arrhenius plot of Si in a crevice/confined space arrangement. Corrosion rate measured in the confined area at different temperatures, from [2].

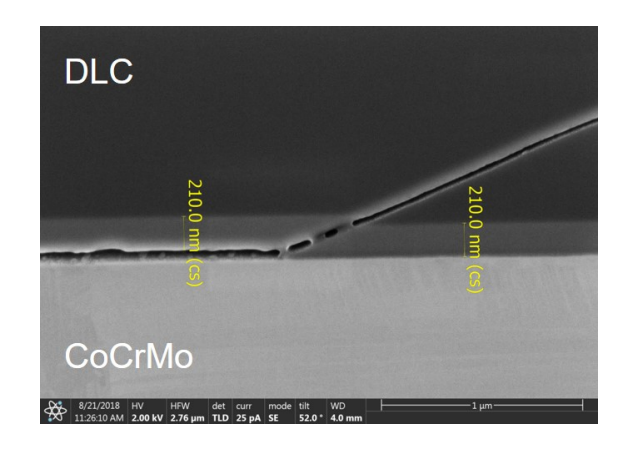


Fig. 2: FIB cross section of a growing crack in 4 µm DLC/Si-DLC (1.0 % O₂ contamination)/ CoCrMo after 13500 cycles in PBS. Plastic deformations of the Si-DLC are visible [3].

DISCUSSION & CONCLUSIONS: The temperature dependent corrosion rates yielded a linear Arrhenius relation, indicating a single rate limiting process step, with the activation energies (Ea) of 106 kJ/mol in 0.01 M PBS, and 109 kJ/mol in Hyclone®. The corrosion rate at 37 °C in PBS is lower than expected, leading to false lifetime expectations. This may be because conditions are not harsh enough, so passivation of Si is still effective and crevice conditions could not (yet) build up. Corrosion was most prevalent at the edge of the crevices, and pH indicators showed a pH increase, potentially due to oxygen reduction inducing OH- release. Concerning corrosion fatigue at the interface, Wöhler curves for different interfaces are generated, showing the deteriorating influence of small interface contaminations. The induced plastic deformations are visible in figure 2, and result in a slowly ongoing local weakening of the material strengths.

REFERENCES: ¹E. Ilic et al., Surface & Coatings Technology, 375 (2019) 402-413. ²E. Ilic, et al., Journal of the Electrochemical Society, 166 (2019) C125-C133. ³A. Pardo, et al., Science and Technology of Advanced Materials, 20 (2019) 173-186.

Implants surface modification: a reliable biomimetic approach

A. Carino⁶, E. Mueller², M. de Wild³, F. Dalcanale³, J. Köser³, W. Moser⁴, B. Hoechst⁵, S. Göddeke⁵, S. Berner⁶, P. Gruner⁶, A. Testino¹

¹Paul Scherrer Institut, ENE-LBK, Villigen, CH, ² Paul Scherrer Institut, BIO-EMF, Villigen, CH, ³ School of Life Sciences FHNW, Institute for Medical Engineering and Medical Informatics, Muttenz, CH, ⁴ Atesos Medical AG, Aarau, CH, ⁵ Hager & Meisinger GmbH, Neuss, DE, ⁶ Medicoat AG, Maegenwill, CH

INTRODUCTION: Dental implants coated with bioactive ceramics are available on the market. Nevertheless, our cost-effective protocol for Ti surface modification aims to accelerate osseointegration and mitigate the temporary weakness in implant stability that occurs a few weeks after implantation. The implant surface is activated with a thin CaP layer using a wet biomimetic route [1].

METHODS: The here developed NanoCoat surface modification is applied to sandblasted and acid-etched surfaces, which are considered as the gold standard in the field. The NanoCoat protocol consists of a multi-step treatment, which generates a thin (~1 um), chemically bonded nanoporous layer of Ti-based ceramics on the metal surface. Synthetic bone (calcium phosphate) is then grown on the surface in biomimetic conditions, according accelerated controlled method [1]. deposition does not suffer from the line-of-sight issue, as well as does not mask the pristine microroughness.

RESULTS: In-vitro tests were comparatively conducted on ø14 mm Ti discs featuring different surface modification: machined, sandblasted and acid-etched (SLA), surface with grafting layer (GL) obtained by chemical and thermal treatments, and the final NanoCoat surface [1]. Biocompatibility was tested with osteosarcoma MG63 human cells. investigated cytotoxicity and alkaline phosphatase activity for osteoblast differentiation. On the NanoCoat surface, MG63 cells proliferated at the same rate as on control (SLA) titanium surfaces and exhibited a healthy, spread morphology (Fig. 1). The alkaline phosphate activity (ALP) after two weeks, as an indicator of osteoblastic (bone-like) differentiation calibrated to protein content, was evaluated as well. The results demonstrate differences among the four surfaces (Fig. 2), whereby the NanoCoat surface features an osteoblastic differentiation with ALP activities twice as high as the gold-standard benchmark (i.e., SLA).

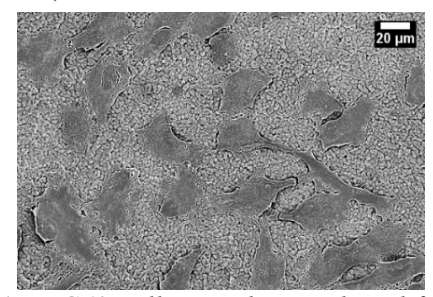


Fig. 1: MG63 cell spreading and proliferation on a substrate with NanoCoat surface.

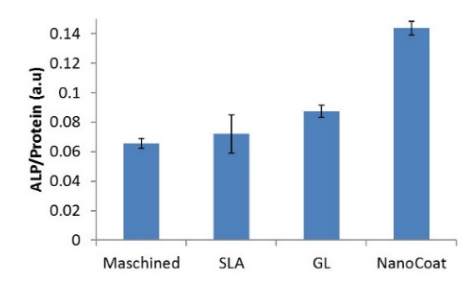


Fig. 2: Comparative ALP assay carried out on four different substrates. The error bars correspond to $\pm SD$.

DISCUSSION & CONCLUSIONS: The experimental results combined with the observed process stability show the ability of the NanoCoat technology as a potential surface treatment for dental implants. The bioactive surface modification, applied as a showcase on dental screws, can further be used on any Tibased permanent implant, such as craniomaxillofacial, spinal, and orthopaedic implants.

ACKNOWLEDGEMENTS: We thank the Swiss Nanoscience Institute and Medicoat AG for the financial support, and Hager & Meisinger for supplying the implants.

REFERENCES: ¹A. Carino, et al. (2018) Formation and transformation of calcium phosphate phases under biologically relevant conditions: Experiments and modelling, Acta Biomaterialia 74: 478.

ICP-MS trace element analysis of calcium phosphate bone substitute materials according to USP 232/233 guidelines

R. Wirz, Y. Viecelli, C. Stähli, M. Bohner *RMS Foundation, Bettlach, CH*

INTRODUCTION: Bone substitute materials B-tricalcium phosphate hydroxyapatite must fulfil the requirements of ISO 13175-3:2012. One fundamental change that will occur once the revised version of this standard has been approved is that the impurity limits set by the standard are not concentrationbased anymore (e.g. maximum 50 ppm heavy metals), but release-based (maximum tolerable daily exposure). This is a paradigm shift in the way the biocompatibility of a bone graft substitute is assessed, but is in line with recent changes introduced for the biological assessment of medical devices (e.g. ISO 10993). The revised ISO 13175-3 standard will request to determine the impurity levels of β-tricalcium phosphate and hydroxyapatite according to the United State Pharmacopeia (USP) chapters USP (product-specific risk analysis) and USP 233 (test validation). The two USP chapters were written based on the recommendations of the International Council for Harmonization (ICH O3D) and therefore are not only decisive for the USA, but also for other authorities, in particular the European. Standards as ASTM and ISO start to refer to the new USP guidelines as well. RMS Foundation has faced a number of new challenges during this method validation using since ICP-MS element the threshold concentrations drop significantly when more implant material biodegrades in a shorter amount of time (consequence of the product specific risk analysis).

METHODS: Inductive coupled plasma mass spectrometry (ICP-MS) is an extremely sensitive technique that allows simultaneous quantification of all target heavy metal elements in calcium phosphates (CaPs) down to trace levels in the μ g/L or sub- μ g/L range. Target elements according to USP 232 are: Cd, Pb, As, Hg, Co, V, Ni, Tl, Au, Pd, Ir, Os, Rh, Ru, Se, Ag, Pt, Li, Sb, Ba, Mo, Cu, Sn, and Cr.

RESULTS: According to USP 233, quantification of heavy metals has to be proven

by showing an accuracy between $70-150\,\%$ at the target concentration of the corresponding heavy metal element. Within this validation study, it could be shown that this requirement could be met (Fig. 1). The corresponding target concentrations based on the performed risk analysis for CaP bone substitute materials had a range as low as $0.08\,\mu\text{g/L}$ for Cd up to $60.00\,\mu\text{g/L}$ for Mo.

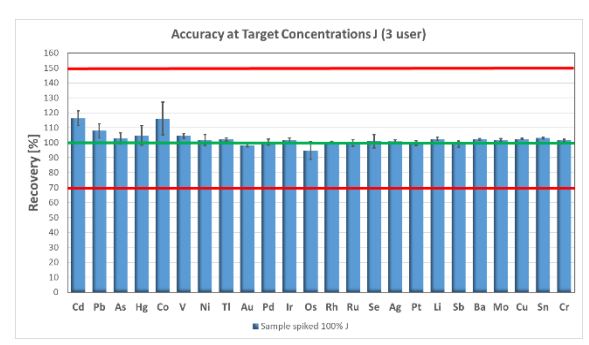


Fig. 1: Recovery rate of the 24 target elements at the target concentrations achieved at the RMS laboratory.

DISCUSSION & **CONCLUSIONS:** The resulting LODs were at least 3 times lower (LOD for Co: $0.066~\mu g/L$) than the respective threshold limit (Co: $0.2~\mu g/L$). The least sensitive analyte was copper with a validated LOD of $0.179~\mu g/L$. In conclusion, the method meets the requirements of USP 232 and USP 233 when testing the elemental impurities present in calcium phosphate products according to a risk assessment assuming 2.875~g of CaPs dissolved in the body per day.

REFERENCES:

USP <232> Elemental Impurities – Limits, in: United States Pharmacop. Natl. Formul. (USP 38-NF 33), United States Pharmacopeia Convention, 2012: pp. 245-248.

USP <233> Elemental Impurities – Procedures, in: Second Suppl. to United States Pharmacop. Natl. Formul. (USP 38-NF 33), United States Pharmacopeia Convention, 2012: pp. 243-244.

Laser Additive Manufactured hemi-thoracic cage custom implant in Ti6Al4V

M. Tomaselli, S. Rappo, P. Robotti *Lincotek Trento S.p.A*, *Pergine Valsugana (TN)*, *IT*

INTRODUCTION: Artificial hemi-thoracic cage reconstruction is a challenging task because of the geometrical complexity, the large dimension of the whole part and the necessary elasticity of the component subjected to cycling deformation to accommodate the chest expansion during the breathing. Additive Layer Manufacturing (ALM) was the preferred choice to fabricate the part. The patient specific shape

can be replicated feeding an Additive

Manufacturing (AM) equipment with a 3D

model obtained through CT-scan images

segmentation.

Design for Additive Manufacturing (DFAM), specific 3D printing process selection and set up, post processing and geometrical controls are all key engineering capability for successfully deliver such a complex implantable component.

MATERIALS & METHODS: The 3D model of the component was obtained through DICOM and segmentation at the Biomedical Engineering Department, Canary Islands Institute of Technology.

In the DFAM stage Materialise E-stage Software was used. The component was made of Ti6Al4V alloy. 3D printing was attempted using a Concept Laser M2 or, in alternative, an EOS M290 ALM equipment.

Two different types of recoaters were tested: soft (silicon wiper) on the M2 equipment and medium (carbon comb) on the M290 equipment. Post processing applied: Heat treatment in vacuum over the beta-transus temperature, band saw detachment, manual supports removal and deburring, surface smoothing by glass beads blasting.

The geometrical conformity between nominal and actual shape was assessed using a fully-integrated laser scanner. The non-contact measurement method acquires a cloud of points to map the surface of the component.

RESULTS & DISCUSSION: The Software helped to define the best support strategy able to minimize the time for AM, suggesting the support dimensions and the part orientation during building (Fig. 1). Moreover, it helped in

minimizing the necking connections between the supports and the part in order to decrease the finishing work. These design choices are in trade off with the opposite necessity to increase the supports and connections dimensions to hold the part in the desired position during the building, nevertheless the local thermal stresses.

The two recoaters tested exhibited different friction forces against the component during the powder spreading. The run with the medium type recoater failed because it caused breaks in the supports. The part swelled and the recoater impinged leading to job crash. By opposite the soft recoater was successful, enabling the part manufacturing along with the use of light supports structures and connections thus minimizing the following post processing steps. Based on the equipment set up and parameters used, the print of the hemi-thoracic cage implant was successfully completed with the M2 machine. This process reached also a native smoother surface finishing.

After AM, the thermal treatment was essential to guarantee the conformity of the mechanical performances and the microstructure with the ASTM F3001, the norm applicable for the implantable grade Ti6Al4V ELI through ALM. After glass bead blasting, the Ra detected on the solid surface of the part was $< 3~\mu m$.

The Laser scanner was a suitable tool enabling fast and precise dimensional quality control for such a complex custom implant.



Fig. 1: ALM Hemi-Thoracic cage in Ti6Al4V.

ACKNOWLEDGEMENTS: This work is part of FAMAC Research Project, partially funded by Provincia Autonoma di Trento, Italy.

Protective pink coating for dental implant applications

N.K. Manninen, S. Guimond, C. Acikgoz

Oerlikon Surface Solutions, Zweigniederlassung Balzers, Technology & Service Center, Balzers, LI

INTRODUCTION: Physical vapor deposited (PVD) coatings are widely used in the dental market for aesthetic reasons. The most common materials in this given application are TiN coatings and diamond-like carbon (DLC) coatings due to their aesthetic properties combined with biocompatibility and their wear resistance. Currently new challenges are imposed by the market, especially regarding the aesthetic properties of dental implants, therefore the main goal is to achieve colours similar to gingiva (gum), skin and teeth. In this context, TiCN based coatings are regarded as a promising coating material due to their inherent pink colour.

METHODS: TiCN coatings with a pink colour have been produced by (Scalable Pulsed Power Plasma) S3p technology. The coatings are characterised in terms of structure by X-ray diffraction (XRD) and chemical composition by electron dispersive spectroscopy (EDS) and elastic recoil detection analysis (ERDA). The coatings topography is also analysed in comparison to arc coatings by scanning electron microscopy (SEM) and profilometry. The colour stability in corrosive environments is also reported, for which the coatings were immersed in 25 wt.-% NaCl solution for 34 days. The substrate materials were made of Ti6Al4V alloy and SS316L. The saline solution was refreshed every 7 days, and the colour was measured by spectrophotometry in order to determine the CIE L*a*b* colour parameters. The variation of colour of as-deposited coating and coating immersed in saline solution is determined by the calculation of ΔE parameter. The samples were also visually inspected by optical light microscopy in order to evaluate the presence of corrosion.

RESULTS: BALIMED TICANA consists of a multilayer coating featuring 3 layers of TiCN with gradual increase in carbon content, ranging from 3 at.-% up to 10 at.-%, as determined by EDS and ERDA. The chemical composition and

texture in the top layer provide the characteristic pink colour. The coating consists of a fcc-TiCN structure, as determined in XRD analysis. The use of S3p technology provides a clear advantage over arc evaporation technology since the number of droplets and particles is largely reduced. The coating shows a stable colour (Δ E=0.7) after 34 days of immersion in solution with 25 wt.-% NaCl without any sign of localized corrosion.

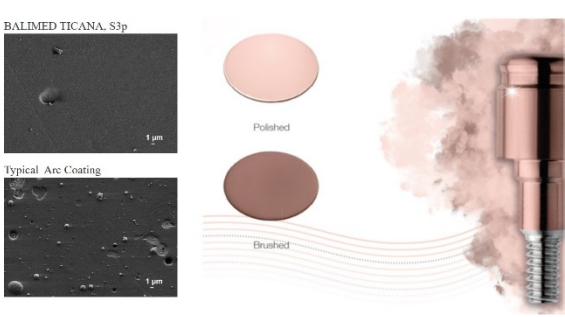


Fig. 1: Scanning electron microscopy (SEM) top view micrographs with comparison of S3p BALIMED TICANA and typical arc coating. Picture of colour achieved with BALIMED TICANA on dental abutment.

DISCUSSION & CONCLUSIONS: BALIMED TICANA is a multilayer TiCN-based coating with pink colour, obtained via introducing a carbon content of 3 at.-% to 10 at.-%. The coating is deposited by S3p technology, providing highly smooth surface combined with high level of hardness.

REFERENCES

¹Kurapov Denis, Krassnitzer Siegfried, TiCN having reduced growth defects by means of HiPIMS, EP 3445890 B1, European Patent, 21 April 2017. ²Krassnitzer Siegfried, Kurapov Denis, High-power pulse coating method, US10392694B2, USA Patent, 27 August 2019. ³BALIMED TICANA, Oerlikon Balzers, Accessed in March 2021, Available Online: https://www.oerlikon.com/balzers/se/en/portfoli o/balzers-surface-solutions/pvd-and-pacvd-based-coatings/balimed/balimed-ticana

Cleanliness of Orthopaedic Implants According to ISO 19227: Differences and Gaps Compared to ISO 10993-18

S. Rohrer¹, R. Heuberger¹, B. Dhanapal²

¹ RMS Foundation, Bettlach, CH, ² Zimmer GmbH, Zimmer Biomet, Winterthur, CH

INTRODUCTION: The evaluation of the cleanliness and biological safety of an orthopaedic implant is a central part of the conformity assessment procedure for market approval. There are two documents describing the cleanliness: ISO 19227 coming from the cleaning processes development and validation and ISO 10993-18 describing the chemical characterisation of medical device materials for the biological evaluation.

In this work, we have taken a closer look at the differences and gaps with regard to the evaluation of the cleanliness of implants.

METHODS: The two standards were compared in terms of their recommendations to test implant cleanliness. Differences and gaps were reported.

RESULTS & DISCUSSION: An important difference is that ISO 19227 focusses on extractable contaminants, while in ISO 10993-18 the investigations can start with the characterization of bulk and surface properties, including leachable and extractable contaminants.

Both standards mention the importance of a risk assessment based on the analysis of the contaminants. However, a limit value of 0.5 mg/implant of total hydrocarbon and organic carbon (THC & TOC) is mentioned in ISO 19227. Although it is mentioned, that this value "can serve as a starting point for acceptance levels", this does not make sense from a toxicological evaluation point of view and could give manufacturers a false sense of security if they follow this example. For example, the threshold of toxicological concern (TTC) for carcinogenic substances, which could be released from a long-term contacting medical device (> 10 years), is 1.5 µg/day (according to ISO/TS 21726). Therefore, limit values have to be determined in a case by case risk assessment. depending on the implant type, site of implantation and exposure or based on the historical clinical performance of the device.

This brings us to the next topic that is missing in ISO 19227, the analytical evaluation threshold (AET) concept. The AET is the concentration

threshold below which extractables or leachables identification is not required. Thus, the chosen analytical method requires a quantification limit that is lower than the AET. This is often not the case with THC and TOC, if used as stand-alone methods.

CONCLUSIONS: ISO 19227 is very helpful in the development and validation of a cleaning process. The proposed analytical methods TOC and THC can be potentially useful for process control of an established cleaning process. However, the list of possible test methods is not sufficiently comprehensive. Focusing on specific examples of test methods and giving suggestions on how to derive an acceptance criterion could give a false sense of security.

A general acceptance limit of 0.5 mg/implant is not appropriate, as the size, complexity, manufacturing and cleaning process of implants are diverse. Thus, limit values have to be determined in a toxicological risk assessment and are usually supplemented by the requirement that the device is visually clean.

Therefore, we suggest that the chemical characterisation of orthopaedic implants should be performed according to ISO 10993-18. Surface contamination is then considered and evaluated as part of the chemical characterisation. If necessary according to the risk mitigation plan, even small amounts of contamination should be identified quantified. If the toxicological assessment shows that the surface contamination is problematic, the cleaning process must be improved in accordance to ISO 19227.

REFERENCES: ISO 19227:2018-03: Implants for surgery - Cleanliness of orthopedic implants - General Requirements. ISO 10993-18:2020-01: Biological evaluation of medical devices - Part 18: Chemical characterization of medical device materials within a risk management process. ISO/TS 21726:2019-02: Biological evaluation of medical devices - Application of the threshold of toxicological concern (TTC) for assessing biocompatibility of medical device constituents.

Dry mechanical-electrochemical polishing of titanium

S. Simeunovic, D. Mory, D. Seiler, M. de Wild

University of Applied Sciences Northwestern Switzerland, FHNW, Muttenz, CH

INTRODUCTION: The post-processing of metallic implants has been given more attention with the continuing rise of additively manufactured (AM) implants. In response to the growing demand, novel automated methods for electropolishing [1] have entered the market in recent years. One such method is the electropolishing process known as *DLyte*, used e.g. for 316L stainless steel [2]. The aim of this study is to assess the post-processing quality of this process on AM cranial titanium plates. Foremost, the influence of process times on the roughness was investigated using conventionally produced rods made of titanium.

METHODS: *Manufacturing of the samples:* Conventionally produced titanium grade 5 rods (Bibus Metals AG) served for roughness tests. Each rod contained four sections where the surface has been roughened, rough machined, fine machined or mechanically polished. AM cranial titanium plates were manufactured by Selective Laser Melting (SLM) using a SLM Solutions 250^{HL} system (SLM Solutions, Lübeck, Germany). The powder used for this process was titanium grade 2 (Realizer GmbH, Borchen, Germany). Post-processing: Each manufactured sample was dry polished using the DLyte H10 (DLyte, Barcelona, Spain) in combination with DLyte TI MIX as the electrolyte. The samples were mounted to metallic specimen holder acting as the anode. The samples were then inserted into the polymeric electrolyte and polished for 90 min in total with 15 min processing intervals between analysis. The voltage during the polishing was fixed to 35 V with the polarity as a cyclic factor.

RESULTS & DISCUSSION: The roughness R_a was lowered significantly throughout all four surface sections of the Ti rods as seen in fig. 1. The R_a value of the fine machined titanium surface was reduced from 0.43 μ m to 0.09 μ m within 90 min processing time. The polished and rough machined surfaces exposed a similar smoothing trend whereas the roughened surface reduced more linearly from R_a 1.17 μ m to R_a 0.77 μ m within 90 min treatment.

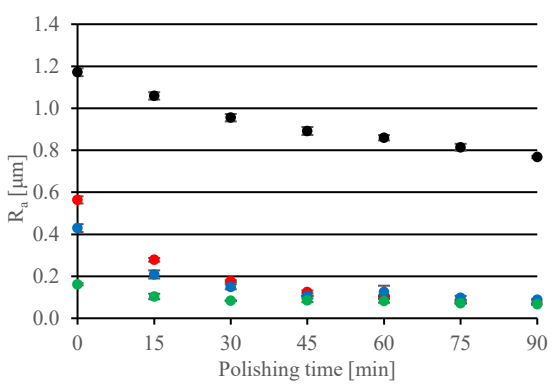


Fig. 1: Decrease of R_a as a function of the polishing time of the roughened (**black**), rough machined (**red**), fine machined (**blue**) and mechanically polished (**green**) surface.

The AM cranial plates showed a significantly improved surface quality as seen in fig. 2. With the DLyte post-treatment the surface has become overall smoother, shiny and with less cavities.

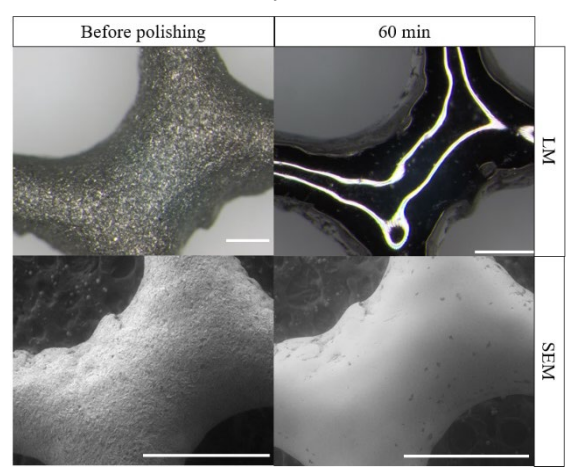


Fig. 2: LM and SEM images of a sandblasted AM titanium strut before polishing (left column) and 60 min polishing time (right column) (scale 1 mm).

CONCLUSIONS: The DLyte technology improved the surface quality of the tested titanium rods especially in cases where the samples had a low R_a value beforehand. The DLyte process has shown great potential in the post-processing of AM titanium implants.

REFERENCES: ¹D. Landolt, et al., Electrochimica Acta 48, 3185-3201 (2003). ²Y. Bai, et al., Materials and Design 193 (2020), 108840.

Adaptive Density Minimal Surfaces for 3D-printed Implants

C. Waldvogel¹, N. Arn¹, P. Malgaroli², D. Seiler², M. de Wild²

¹ spherene AG, Zürich, CH,

² University of Applied Sciences Northwestern Switzerland, FHNW, Muttenz, CH

INTRODUCTION: While an increasing range of possibilities for 3D-printed medical implants is implied by the latest 3D design and engineering methods, they are far from unlocking the full potential offered by this new production route, failing to address main requirements on the internal structure of implants, whilst maintaining structural stability: easy access for cleaning, maximum surface area for osseointegration or internal coatings with slowly degrading substances, open-porous structures allowing high fluid-flow for fast vascularization and bone growth. Also, the impact of suboptimal design on the additive manufacturing of titanium implants limits their competitiveness toward traditionally produced implants: tedious removal of support structures, thus non-controllable surface texture and residues from mechanical removal, and shape sacrifices to avoid closed powder pockets.

Additive manufacturing offers new possibilities for a *change of minds* in the design of medical implants thanks to the (relative) freedom of shape and the *complexity for free* ruleset, thus paving the way for implants where all of the afore-mentioned requirements are addressed.

METHODS: To this purpose we developed a freely configurable 3D-structure with an *Adaptive Density Minimal Surface* geometry (ADMS), which is able to computationally emulate both the plate- and rod-type geometry of trabecular bone (Fig. 1), as well as the near-solid cortical bone. ADMS structures feature open channels through the entire implant, maximized inner surfaces and allow for support-free printing and easy cleaning [1].

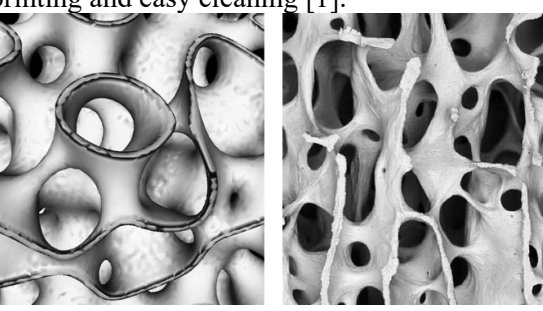


Fig. 1: ADMS geometry (left) vs. trabecular bone structure.

RESULTS: Locally configurable ADMS parameters include load case, thickness, channel diameter and porosity or structural density. As *minimal surfaces*, ADMS exhibit a smooth curvature distribution and are thus exceptionally stable using the minimal amount of material [1].

A variety of ADMS samples with different gradients applied on structural density and surface thickness have been designed. On both top and bottom, solid endplates have been added for a defined load application during mechanical testing.



Fig. 2: Support-free 3D-printed titanium samples with different generation parameters.

The designed ADMS-samples have been 3D-printed by Selective Laser Melting (SLM) on a SLM Solutions 250^{HL} system (SLM Solutions, Lübeck, Germany) out of titanium grade II powder with a d₅₀-value of 40 µm (Fig. 2). We were able to show that all proposed ADMS sample structures can be successfully manufactured by SLM without build supports.

DISCUSSION & CONCLUSIONS: It was shown that scaffolds based on ADMS microarchitectures can be successfully produced out of titanium by SLM. In particular, support structures are not necessary, which is of great advantage during production and post-treatment.

ACKNOWLEDGEMENTS: This study was supported by Innosuisse: grant 43760.1 IP-LS.

REFERENCES: ¹ Patents PCT/IB2019/ 054076, PCT/EP2020/063727.

Post-treatment of wear protection layer

F. Schuler¹, C. Grünzweig², C. Chan Sin Ting², N. Casati², M. Olbinado², A. Carmona¹, M. de Wild¹

¹ University of Applied Sciences Northwestern Switzerland <u>FHNW</u>, Muttenz, CH, ² ANAXAM, PARK INNOVAARE: deliveryLAB, Villigen, CH

INTRODUCTION: The aim of the proprietary plasma-sprayed wear protective layer is to extend the life of titanium surfaces which are subject to abrasion wear. The rather limited wear-resistance of titanium parts could be compensated by a hard ceramic plasma-sprayed coating, in particular on sliding surfaces [1]. Therefore, a novel multicomponent Al₂O₃/TiO₂ powder mixture as starting material is injected in the plasma flame, where the particles melt. On the flight to the sandblasted implant surface, the droplets start to cool down before they impact the substrate with high kinetic energy. There they immediately solidify under high cooling rates forming the multi-component surface coating. This thermal quenching is the reason for the formation of not fully ceramized, non-stoichiometric, partially electrically oxygen-deficient, conductive, crystalline phases and for the appearance of pores and micro cracks [2]. We identified under what conditions these phases form and how they can be subsequently transformed.

METHODS: Vickers HV1 hardness (Zwick-Roell, Germany), SEM (TM3030, Hitachi) and XRD measurements (Bruker Phaser D2 diffractometer, in Bragg-Brentano geometry) were done on polished, anodized and heat-treated single and mixed Al₂O₃/TiO₂ coatings (Fig. 1). High-resolution Synchrotron X-ray microcomputed tomographic SXRμCT measurement were performed with 1 mm2 cut strips from post-treated samples to inspect the coating and the interface between the coating and the Ti grade 5-substrate.



Fig. 1: Cross-section preparation with diamond saw and ion-milling for SEM investigations.

RESULTS: While anodization showed only little effect, the hardness significantly increased after thermal oxidation (Fig. 2a). Crystallographic analysis showed a clear change in the phase composition. Oxidation of non-stoichiometric phases and reduction of high temperature phases was observed in the thermally treated samples (Fig. 2b). XRD indicates that thermal treatment induces transformation into rutile. This also

explains the increase in hardness after post-treatment.

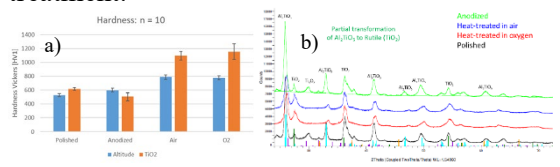
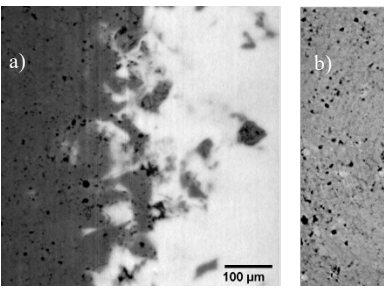


Fig. 2: a) HV1- and b) XRD-measurement after different post-treatments.

With SXRµCT several features were found at the interface and in the coating (Fig. 3): 1) A rippled interface, having a coating-substrate interlayer with thickness ~40 µm, 2) an agglomeration of pores near the interface, 3) smaller pores in the coating, 4) different grey levels inside coatings due to different intensity measured. The variation in intensity in distinct volumes can be caused by different phases present inside the coatings.



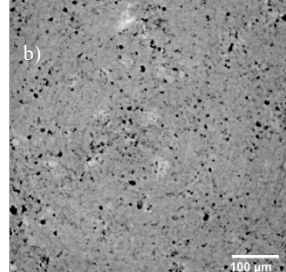


Fig. 3: a) Reconstructed SXR μ CT images of the substrate- Al_2O_3 coating interface. b) Reconstructed cross-section through the Al_2O_3 coating.

DISCUSSION & CONCLUSION: Appropriate heat treatments seem to have a positive influence on the multi-component Al2O3/TiO2 wear protection layer in terms of mechanical, structural, crystallographic and tribological properties.

REFERENCES: ¹ N. Vogt, K. Wozniak, A. Salito, M. de Wild, Biocompatible wear-resistant VPS coatings, Current Directions in Biomedical Engineering 2(1): 31–34 (2016). ² A. Richter, et al. Emergence and impact of Al₂TiO₅ in Al₂O₃-TiO₂ APS coatings. IOP Conf. Ser.: Mater. Sci. Eng. 480 012007 (2019).

ACKNOWLEDGEMENTS: We would like to thank the Swiss Nano Sciences Institute SNI and Nanoargovia for their support of the project.